fractal and fractional

MDPI

Article

Synchronization of Fractional Chaotic Systems with Time-Varying Perturbation

Shaofu Wang

School of Information and Management, Guangxi Medical University, Nanning 530021, China; wangshaofu@gxmu.edu.cn

Abstract

Aiming at the synchronization problem of fractional time-varying perturbation systems, an improved WRBF neural network was proposed based on the wavelet function and radial basis function (RBF). Then, the adaptive controller and updated law are derived based on the WRBF network. It is used to approximate functions and adjust the corresponding parameters in the controller. Based on Lyapunov and Barbalat stability theory, the synchronization of a fractional system with time-varying perturbation is proved effectively.

Keywords: fractional chaotic system; synchronization; WRBF; neural network; time varying perturbation

1. Introduction

With the continuous development of technology, the application of fractional calculus in engineering practice and physics has become a hot topic [1–5]. With the upsurge of studying fractional calculus which has been extended to chaotic systems, fractional chaotic systems have seen broad applications in image encryption [6], electrical circuit [7], secure communication [8], biomedical [9], neural network [10], and other fields. Synchronization is one branch of nonlinear science [11], its application scope includes quantum communication [12], biological neural network [13], physical internet [14], etc. Various synchronization control methods have been proposed, which mainly include parameter identification method in [15], hybrid projective combination synchronization method in [16], adaptive sliding mode control approach in [17], Lyapunov-based approach in [18], H^{∞} synchronization approach in [19], fuzzy feedback control method in [20], modified projective function synchronization method in [21], active parameter identification method [22], etc. The above methods are all about synchronization of fractional systems. Whether they are suitable for fractional uncertain chaotic systems with external disturbances remains to be studied.

From the practical perspective, the fractional chaotic system is of practical significance for investigating dynamical behavior and its synchronization. In Ref. [23], a parameter identification controller is designed to obtain the synchronization of isomer system in the case of multiple disturbance terms, which realizes combined synchronization in a finite time. Ref. [24] uses the idea of multi-switch sliding mode control to directly eliminate nonlinear terms and realizes the combined synchronization of fractional system with external interference, but its control cost is relatively high. In Ref. [25], the inverse matrix method was used to realize passive synchronization of a fractional memristive neural network. However, the controller needs to know the coefficient matrix of the linear part between the driving and response systems, which is highly dependent on the system model. When there are uncertainties or external disturbances, the method finds it difficult

check for updates

Academic Editors: Bruce Henry and David Kubanek

Received: 10 August 2025
Revised: 18 September 2025
Accepted: 19 September 2025
Published: 22 September 2025

Citation: Wang, S. Synchronization of Fractional Chaotic Systems with Time-Varying Perturbation. *Fractal Fract.* **2025**, *9*, 618. https://doi.org/10.3390/fractalfract9090618

Copyright: © 2025 by the author. Licensee MDPI, Basel, Switzerland. This article is an open access article distributed under the terms and conditions of the Creative Commons Attribution (CC BY) license (https://creativecommons.org/licenses/by/4.0/).

to achieve synchronization. Ref. [26] uses a fuzzy control method to realize fixed-time synchronization. However, the design of this controller is complicated, which is not conducive to its implementation in engineering. In Ref. [27], a discrete time-varying observer was designed to obtain the impulse synchronous control of fractional systems in the case of multiple disturbance terms. The observer realized impulse synchronization. In addition, all the above control methods are based on uncertain or unknown systems, or there is aging and decay of components in the operation process of the system. The above factors make the ideal model. On the one hand, the RBF neural network has been proven to approximate any continuous function [28,29]; based on the above considerations, this manuscript mainly studies the synchronous control of uncertain fractional chaotic systems based on an improved RBF neural network and Wavelet function, that is, wavelet radial-based function neural network. The asymptotic synchronization of a fractional uncertain chaotic system is realized. The novelty in the manuscript under review is on the focus of two parts:

(1) An improved RBF neural network with a wavelet function is proposed.
(2) Based on the Barbalat lemma, an adaptive WRBF neural network controller and adaptive law are designed. The designed controller can obtain the synchronization of fractional systems under the condition of external disturbance.

2. Preliminaries

Definition 1 ([30]). *The Caputo transformation is described as*

$$ {}_0^C D_t^{-q} f(t) = \int_0^t (t-\tau)^{q-1} f(\tau) d\tau / \Gamma(q), \tag{1} $$

The fractional derivative of Caputo [30] is

$$ {}_0^C D_t^{q} f(t) = \frac{1}{\Gamma(n-q)} \int_0^t \frac{f^{(n)}(\tau)}{(t-\tau)^{q+1-n}} d\tau, \tag{2} $$

where $\Gamma(z) = \int_0^\infty t^{z-1} e^{-t} dt$, and n denotes n-order.

The structure of WRBF [29–32] is depicted in Figure 1.

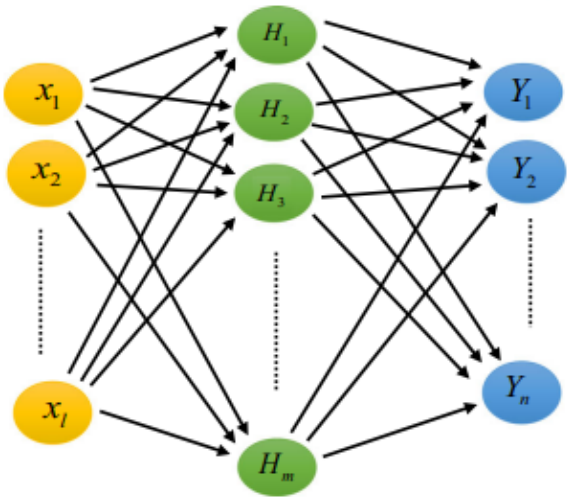

Figure 1. The structure of WRBF [29–32].

$H_i(x)$ is given as

$$H_i(x) = \left(1 - \left\|\frac{x-\mu_i}{\sigma_i^2}\right\|^2\right) \exp\left(-\frac{\|x-\mu_i\|^2}{2\sigma_i^2}\right), \tag{3}$$

The output y_j is given as

$$y_j = \sum_{i=1}^{L} w_{ji} H_i(x) = W_j^T H(x), \tag{4}$$

$$\hat{Q} = Q + \varepsilon_\Delta = \sum_{j=1}^{m} \omega_{i,j} H_{i,j}(x) + \varepsilon_\Delta = WH(x) + \varepsilon_\Delta, i = 1, 2, \cdots, n, \tag{5}$$

where $x \in R^n$, $y \in R^m$, $H(x)$ is the output vector, L denotes the number of hidden layers, $W_j = [w_{j1}, w_{j2}, \cdots, w_{jq}]^T$, m denotes the number of output layers, and μ_i and σ_i express the center and width, respectively. Figure 2 shows the responses of WRBF and RBF. The unknown function $Q(t, X)$ will be estimated by the WRBF neural network, in which according to Equation (14), the error of estimation can be expressed as $W_i H_i + \varepsilon_\Delta - \hat{W}H = \widetilde{W}H + \varepsilon_\Delta$.

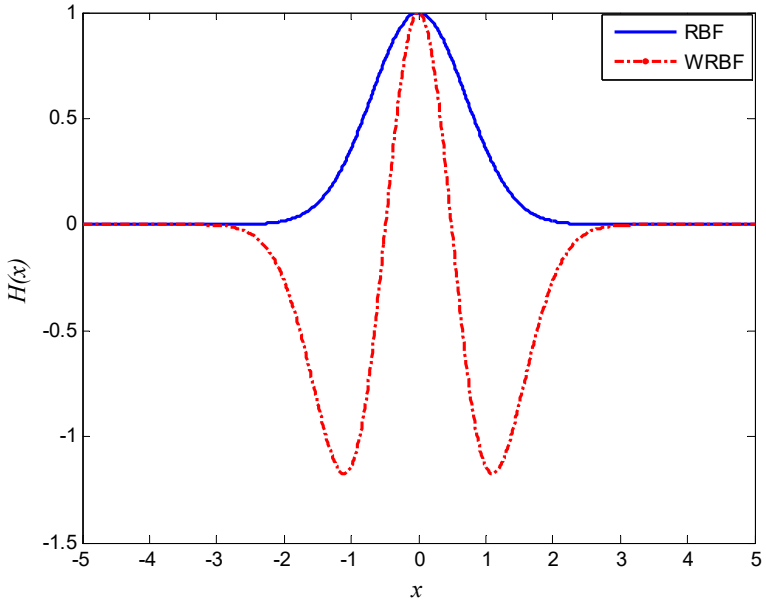

Figure 2. The responses of WRBF and RBF.

3. Synchronization Controller Design

3.1. Description of Synchronization Control Problems

Two fractional systems are considered.

Driven system

$$D_t^q x = f(x) + d_m. \tag{6}$$

Response system

$$D_t^q y = g(y) + d_s + u. \tag{7}$$

where d_m and d_s are external disturbances, $u(t)$ is the controller. The error $e = y - x$. $e = [e_1, e_2, \cdots, e_n]^T$. When $\lim_{t\to\infty} \|e\| = 0$, that is, when the synchronization error asymptotically approaches zero, Systems (6) and (7) can realize synchronization.

3.2. Controller Design with WRBF

The error

$$D_t^q e = g(y) - f(x) + d_s(t) - d_m(t) + u(t), \tag{8}$$

Let

$$Q = g(y) - f(x) + d_s(t) - d_m(t), \tag{9}$$

where Q is an unknown nonlinear function; then, Equation (8) can be rewritten as

$$D_t^q e = Q + u(t), \tag{10}$$

The uncertain function Q is approximated by Equation (5) of the WRBF neural network.

$$\hat{Q}_i = W_i^T H, \tag{11}$$

where W_i is the weight vector of the WRBF network. W_i^* expresses its optimal estimation parameter, and the optimal estimation is

$$\hat{Q}_i^* = W_i^{*T} H, \tag{12}$$

And defining $\overline{W}_i = W_i - W_i^*$, one obtains

$$\dot{\overline{W}}_i = \dot{W}_i, \tag{13}$$

The synchronization controller is designed as

$$u_i(t) = -W_i^T H - \eta_i \mathrm{sgn}[e_i(t)] - \delta_i D_t^{q-1} e_i(t), \tag{14}$$

where η_i is the optimal constant and δ_i is the estimated value of feedback gain δ_i^*. The integer order adaptive laws, the estimated value of the upper bound of optimal approximation error, and the estimated value of feedback gain are, respectively, as follows:

$$\dot{W}_i = k_i [D_t^{q-1} e_i(t)] H, \tag{15}$$

$$\dot{\eta}_i = m_i D_t^{q-1} |e_i(t)|, \tag{16}$$

$$\dot{\delta}_i = n_i [D_t^{q-1} e_i(t)]^2, \tag{17}$$

where $k_i, m_i, n_i > 0$ are the adjusting parameters of the adaptive update laws, respectively.

Theorem 1. *Given the initial conditions, under the action of the designed adaptive WRBF neural network controller (14) and adaptive laws (15)– (17), the synchronization control of (6) and (7) can be realized.*

Proof. The synchronization controller (14) can be substituted into Equation (10), and one has

$$D_t^q e_i(t) = Q_i - W_i^T H - \eta_i \mathrm{sgn}[e_i(t)] - \delta_i D_t^{q-1} e_i(t), \tag{18}$$

According to Equations (5) and (18), one obtains

$$D_t^q e_i(t) = \varepsilon_i - \hat{W}_i^T H - \eta_i \mathrm{sgn}[e_i(t)] - \delta_i D_t^{q-1} e_i(t), \tag{19}$$

where $\varepsilon_i = \phi_i - \hat{\phi}_i$.

Define Lyapunov function as follows:

$$V = \frac{1}{2}\sum_{i=1}^{n}[D_t^{q-1}e_i(t)]^2 + \frac{1}{2}\sum_{i=1}^{n}\frac{1}{k_i}\overline{W}_i^T\overline{W}_i + \frac{1}{2}\sum_{i=1}^{n}\frac{1}{m_i}(\eta_i - \varepsilon_i^*)^2 + \frac{1}{2}\sum_{i=1}^{n}\frac{1}{n_i}(\delta_i - \delta_i^*)^2, \quad (20)$$

where ε_i^* and δ_i^* are constants. The derivative of both sides of Equation (20), one has

$$\dot{V} = \sum_{i=1}^{n}[D_t^{q-1}e_i(t)][D_t^q e_i(t)] + \sum_{i=1}^{n}\frac{1}{k_i}\overline{W}_i^T\dot{\overline{W}}_i + \sum_{i=1}^{n}\frac{1}{m_i}(\eta_i - \varepsilon_i^*)\dot{\eta}_i + \sum_{i=1}^{n}\frac{1}{n_i}(\delta_i - \delta_i^*)\dot{\delta}_i. \quad (21)$$

When Equation (19) and update laws (15)–(17) are substituted into Equation (21), one has

$$\begin{aligned}
\dot{V} &= \sum_{i=1}^{n}[D_t^{q-1}e_i(t)]\left(\varepsilon_i - \overline{W}_i^T H - \eta_i \mathrm{sgn}(e_i(t)) - \delta_i D_t^{q-1}e_i(t)\right) + \sum_{i=1}^{n}\overline{W}^T\left[\left(D_t^{q-1}e_i(t)\right)H\right] + \\
&\sum_{i=1}^{n}(\eta_i - \varepsilon_i^*)\left[D_t^{q-1}|e_i(t)|\right] + \sum_{i=1}^{n}(\delta_i - \delta_i^*)\left[D_t^{q-1}e_i(t)\right]^2, \\
&= \sum_{i=1}^{n}\varepsilon_i[D_t^{q-1}e_i(t)] - \sum_{i=1}^{n}[D_t^{q-1}e_i(t)]\overline{W}_i^T H - \sum_{i=1}^{n}\eta_i\left[D_t^{q-1}|e_i(t)|\right] - \sum_{i=1}^{n}\delta_i\left[D_t^{q-1}e_i(t)\right]^2 \\
&+ \sum_{i=1}^{n}\left[\left(D_t^{q-1}e_i(t)\right)\overline{W}_i^T H\right] + \sum_{i=1}^{n}(\eta_i - \varepsilon_i^*)\left[D_t^{q-1}|e_i(t)|\right] + \sum_{i=1}^{n}(\delta_i - \delta_i^*)\left[D_t^{q-1}e_i(t)\right]^2 \\
&= \sum_{i=1}^{n}\varepsilon_i[D_t^{q-1}e_i(t)] - \sum_{i=1}^{n}\varepsilon_i^*\left[D_t^{q-1}|e_i(t)|\right] - \sum_{i=1}^{n}\delta_i^*\left[D_t^{q-1}e_i(t)\right]^2,
\end{aligned} \quad (22)$$

As $0 \le |\varepsilon_i| \le \varepsilon_i^*$, $D_t^{q-1}e_i(t) \le D_t^{q-1}|e_i(t)|$,

$$\begin{aligned}
\dot{V} &\le \sum_{i=1}^{n}\varepsilon_i^*[D_t^{q-1}e_i(t)] - \sum_{i=1}^{n}\varepsilon_i^*\left[D_t^{q-1}|e_i(t)|\right] - \delta\sum_{i=1}^{n}\delta_i^*\left[D_t^{q-1}e_i(t)\right]^2 \\
&= -\sum_{i=1}^{n}\delta_i^*\left[D_t^{q-1}e_i(t)\right]^2 \\
&= -\sum_{i=1}^{n}\delta\left[D_t^{q-1}e_i(t)\right]^2 \le 0,
\end{aligned} \quad (23)$$

where $\delta = \min\{\delta_1^*, \delta_2^*, \ldots, \delta_n^*\}$. One obtains

$$\frac{1}{2}\sum_{i=1}^{n}\left[D_t^{q-1}e_i(t)\right]^2 \le V(t), \quad (24)$$

Thus, $\frac{1}{2}[D_t^{q-1}e_i(t)]^2 \le V(t) \le V(0)$, $D_t^{q-1}e_i(t)$ is bounded. Similarly, $\overline{W}_i$, η_i, and δ_i are bounded. The integral of the inequality $\dot{V}(t) \le -\sum_{i=1}^{n}\delta[D_t^{q-1}e_i(t)]^2$, one obtains

$$V(t) - V(0) \le -\delta\int_0^t\sum_{i=1}^{n}[D_t^{q-1}e_i(\tau)]^2 d\tau \le -\delta\int_0^t[D_t^{q-1}e_i(\tau)]^2 d\tau, \quad (25)$$

According to Equation (25), $\lim_{t\to\infty}[D_t^{q-1}e_i(\tau)]^2 d\tau \le V(0)/\delta - \lim_{t\to\infty}V(t)/\delta < \infty$, that is, $D_t^{q-1}e_i(t) \in L_2$. As such, one has

$$\left\|D_t^q e_i(t)\right\| \le \left\|\overline{W}_i^T\right\|\|H\| + \varepsilon_i^* + |\eta_i| + |\delta_i|\left|D_t^{q-1}e_i(t)\right|, \quad (26)$$

According to Equation (3), the function $\|H\|$ is bounded and $D_t^q e_i(t)$ is bounded. $D_t^{q-1}e_i(t) \in L_2 \cap L_\infty$ and $D_t^q e_i(t) \in L_\infty$. According to the Barbalat theorem, one has

$$\lim_{t\to\infty}e_i(t) = 0, \quad (27)$$

Thus, the synchronization error asymptotically approaches zero. The proof is finished.

4. Simulation

For simulation, let the fractional chaotic system be

$$\begin{cases} D_t^q x_1 = -ax_1 + x_2x_3 + d_{m1}(t) \\ D_t^q x_2 = cx_1 - ax_1x_3 + d_{m2}(t) \\ D_t^q x_3 = x_1x_2 - bx_3 + d_{m3}(t) \end{cases}, \tag{28}$$

When the parameters $q = 0.91$, $a = 5$, $b = 2$, $c = 34$, initial value $x(0) = [1, 2, 3]^T$. Equation (28) appears chaotic in Figure 3. The bifurcation diagram (BD) of q is shown in Figure 4.

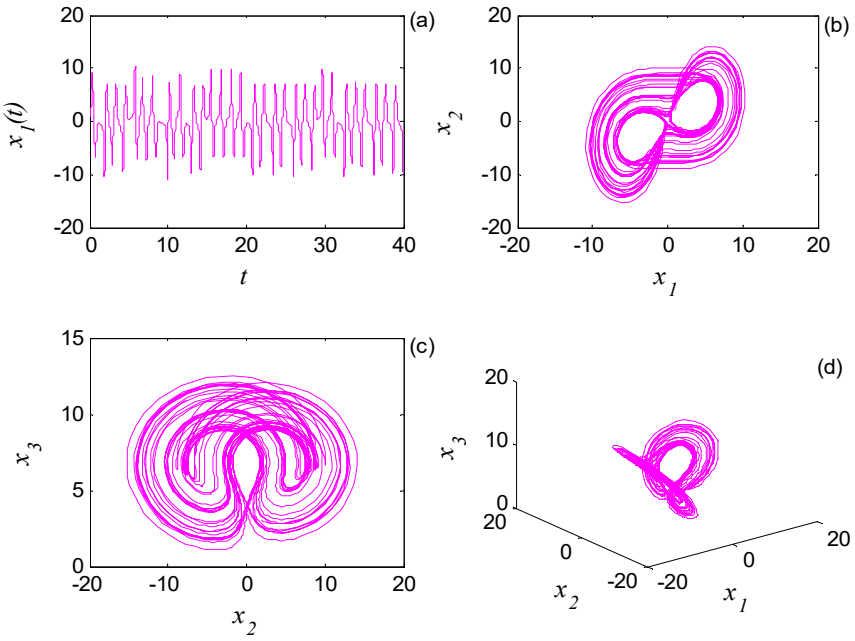

Figure 3. Time-domain response and phase diagrams of Equation (27). (**a**) t, x_1(t),(**b**) x_1, x_2, (**c**) x_2, x_3, (**d**) x_1, x_2, x_3.

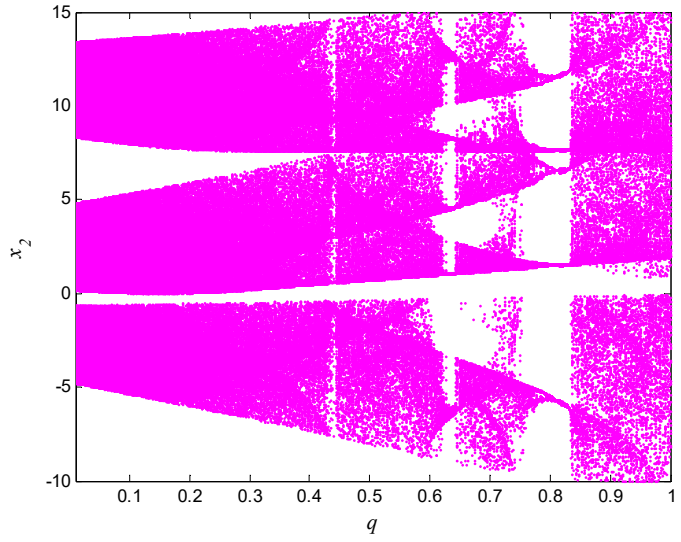

Figure 4. BD of Equation (27) with q.

As the time-varying perturbation is added, the driven system can be described as

$$\begin{bmatrix} D_t^q x_1 \\ D_t^q x_2 \\ D_t^q x_3 \end{bmatrix} = \begin{bmatrix} -5x_1 + x_2 x_3 \\ 34x_1 - 5x_1 x_3 \\ x_1 x_2 - 2x_3 \end{bmatrix} + \begin{bmatrix} 0.1\sin(t) + \cos(t) \\ 0.1\sin(t) + \cos(t) \\ 0.1\sin(t) + \cos(t) \end{bmatrix}, \tag{29}$$

and the response system with time-varying perturbation is given as

$$\begin{bmatrix} D_t^q y_1 \\ D_t^q y_2 \\ D_t^q y_3 \end{bmatrix} = \begin{bmatrix} -5y_1 + y_2 y_3 \\ 34y_1 - 5y_1 y_3 \\ y_1 y_2 - 2y_3 \end{bmatrix} + \begin{bmatrix} 0.2\sin(t) + \cos(2t) \\ 0.2\sin(t) + \cos(2t) \\ 0.2\sin(t) + \cos(2t) \end{bmatrix} + \begin{bmatrix} u_1(t) \\ u_2(t) \\ u_2(t) \end{bmatrix}. \tag{30}$$

In numerical simulation, the hidden layer neuron is set to 9, μ =[−2, −1.5, −1, −0.5, 0, 0.5, 1, 1.5, 2], and the width $\sigma_j = 0.7$, (j =1,2,. . . . .9). Using controller (14) and the adaptive update laws (15)–(17), the adjusting parameters of the adaptive law $k_i = 1$, $m_i = 1$, $n_i = 0.1$, and the weights of the RBF neural network $W_i(0) = 1$. The initial values of the adaptive law $\eta_i(0) = 5$, $\delta_i(0) = 0.1$. From Figure 5, it is observed that the synchronization error converges quickly, which indicates that the designed WRBF neural network has a good approximation effect.

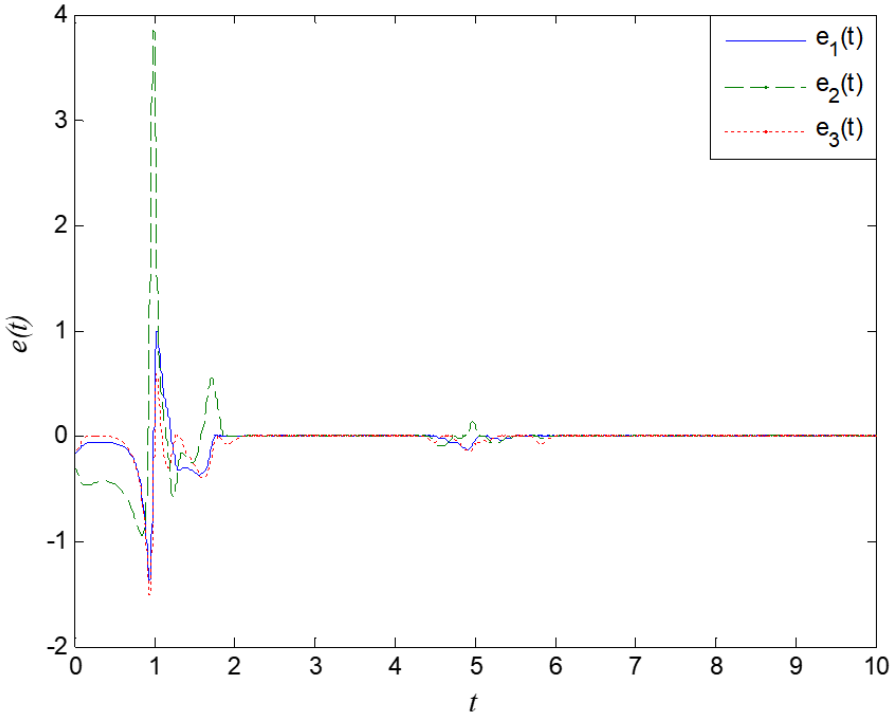

Figure 5. The error e_i between (29) and (30).

5. Conclusions

In summary, an improved RBF neural network using a wavelet function for time-varying perturbation systems was proposed. A controller was designed. In stability analysis, the derivative of the corresponding Lyapunov function was directly used to avoid the fractional derivative, and the error system asymptotically reached zero by using the correlation lemma. The controller designed in this paper is independent of the system model and can realize synchronous control under completely unknown external disturbance.

Funding: This project was supported by the "Four New" Research Fund of Guangxi Medical University, grant number SX202324.

Data Availability Statement: The original contributions presented in this study are included in the article. Further inquiries can be directed to the corresponding author.

Conflicts of Interest: The author declares no conflicts of interest.

References

1. Elwy, O.; Abdelaty, A.M.; Said, L.A.; Radwan, A.G. Fractional calculus definitions, Approximations, and engineering applications. *J. Eng. Appl. Sci.* **2020**, *67*, 1–30.
2. Sun, H.G.; Zhang, Y.; Baleanu, D.; Chen, W.; Chen, Y. A new collection of real world applications of fractional calculus in science and engineering. *Commun. Nonlinear Sci. Numer. Simul.* **2018**, *64*, 213–231. [CrossRef]
3. Das, S. Application of generalized fractional calculus in other science and engineering fields. In *Functional Fractional Calculus*; Springer: Berlin/Heidelberg, Germany, 2011; pp. 437–492.
4. Hernndez-Balaguera, E. Coulostatics in bioelectrochemistry: A physical interpretation of the electrode-tissue processes from the theory of fractional calculus. *Chaos Solitons Fractals* **2021**, *145*, 110787. [CrossRef]
5. Samraiz, M.; Perveen, Z.; Abdeljawad, T.; Iqbal, S.; Naheed, S. On certain fractional calculus operators and applications in mathematical physics. *Phys. Scr.* **2020**, *95*, 115210. [CrossRef]
6. Abdeljawad, T.; Banerjee, S.; Wu, G.-C. Discrete tempered fractional calculus for new chaotic systems with short memory and image encryption. *Opt.-Int. J. Light Electron Opt.* **2020**, *218*, 163698. [CrossRef]
7. Banchuin, R. Comparative analyses of electrical circuits with conventional and revisited definitions of circuit elements: A fractional conformable calculus approach. *COMPEL* **2022**, *41*, 258–282. [CrossRef]
8. Yang, J.; Xiong, J.; Cen, J.; He, W. Finite-time generalized synchronization of non-identical fractional order chaotic systems and its application in speech secure communication. *PLoS ONE* **2022**, *17*, e0263007. [CrossRef]
9. Prommee, P.; Pienpichayapong, P.; Manositthichai, N.; Wongprommoon, N. OTA-based tunable fractional-order devices for biomedical engineering. *AEU-Int. J. Electron. Commun.* **2021**, *128*, 153520. [CrossRef]
10. Yang, X.; Fang, H.; Wu, Y.; Jia, W. RBF neural network fractional-order sliding mode control with an application to direct a three matrix converter under an unbalanced grid. *Sustainability* **2022**, *14*, 3193. [CrossRef]
11. Chang, S.-C. Bifurcation, routes to chaos, and synchronized chaos of electromagnetic valve train in camless engines. *Int. J. Nonlinear Sci. Numer. Simul.* **2021**, *22*, 447–460. [CrossRef]
12. Aliabadi, F.; Majidi, M.-H.; Khorashadizadeh, S. Chaos synchronization using adaptive quantum neural networks and its application in secure communication and cryptography. *Neural Comput. Appl.* **2022**, *34*, 6521–6533. [CrossRef]
13. Zeng, X.; Hui, Q.; Haddad, W.M.; Hayakawa, T.; Bailey, J.M. Synchronization of biological neural network systems with stochastic perturbations and time delays. *J. Frankl. Inst.* **2014**, *351*, 1205–1225. [CrossRef]
14. Leung, E.K.; Lee, C.K.H.; Ouyang, Z. From traditional warehouses to physical internet hubs: A digital twin-based inbound synchronization framework for PI-order management. *Int. J. Prod. Econ.* **2022**, *244*, 108353. [CrossRef]
15. Khan, T.; Chaudhary, H. Combination anti-synchronization for chaos generated by generalized Lotka-Volterra biological systems using parameter identification method. *Math. Eng. Sci. Aerosp.* **2021**, *12*, 383–393.
16. Khan, T.; Chaudhary, H. An investigation on parameter identification method of controlling chaos in generalized Lotka-Volterra systems via hybrid projective difference combination synchronization technique. In *Advances in Mechanical Engineering*; Springer: Singapore, 2021; pp. 547–558.
17. Wang, R.; Zhang, Y.; Chen, Y.; Chen, X.; Xi, L. Fuzzy neural network-based chaos synchronization for a class of fractional-order chaotic systems: An adaptive sliding mode control approach. *Nonlinear Dyn.* **2020**, *100*, 1275–1287.
18. Hai, Q. Sampled-data synchronization control for chaotic neural networks with mixed delays: A discontinuous Lyapunov functional approach. *IEEE Access* **2021**, *9*, 25383–25393. [CrossRef]
19. Pan, L.; He, P.; Li, Z.; Mi, H.; Wang, H. Delay-range-dependent H^{∞} synchronization approaches for time-delay chaotic systems. *Int. J. Comput. Math.* **2021**, *99*, 949–965. [CrossRef]
20. Kumar, S.; Khan, A. Controlling and synchronization of chaotic systems via Takagi-Sugeno fuzzy adaptive feedback control techniques. *J. Control Autom. Electr. Syst.* **2021**, *32*, 842–852.
21. Zhang, F.; Gao, R.; Huang, Z.; Jiang, C.; Chen, Y.; Zhang, H. Complex modified projective difference function synchronization of coupled complex chaotic systems for secure communication in WSNs. *Mathematics* **2022**, *10*, 1202. [CrossRef]
22. Chaudhary, H.; Khan, A.; Nigar, U.; Kaushik, S.; Sajid, M. An effective synchronization approach to stability analysis for chaotic generalized Lotka-Volterra biological models using active and parameter identification methods. *Entropy* **2022**, *24*, 529. [CrossRef] [PubMed]
23. Pan, W.; Li, T.; Sajid, M.; Ali, S.; Pu, L. Parameter identification and the finite-time combination-combination synchronization of fractional-order chaotic systems with different structures under multiple stochastic disturbances. *Mathematics* **2022**, *10*, 712. [CrossRef]

24. Pan, W.; Li, T.; Wang, Y. The multi-switching sliding mode combination synchronization of fractional order non-identical chaotic system with stochastic disturbances and unknown parameters. *Fractal Fract.* **2022**, *6*, 102. [CrossRef]
25. Anbalagan, P.; Ramachandran, R.; Alzabut, J.; Hincal, E.; Niezabitowski, M. Improved results on finite-time passivity and synchronization problem for fractional-order memristor-based competitive neural networks: Interval matrix approach. *Fractal Fract.* **2022**, *6*, 36. [CrossRef]
26. Xiao, J.; Cheng, J.; Shi, K.; Zhang, R. A general approach to fixed-time synchronization problem for fractional-order multidimension-Valued fuzzy neural networks based on memristor. *IEEE Trans. Fuzzy Syst.* **2022**, *30*, 968–977. [CrossRef]
27. Li, R.; Wu, H.; Cao, J. Impulsive exponential synchronization of fractional-order complex dynamical networks with derivative couplings via feedback control based on discrete time state observations. *Acta Math. Sci.* **2022**, *42*, 737–754. [CrossRef]
28. Nian, F.; Liu, X.; Zhang, Y.; Yu, X. Module-phase synchronization of fractional-order complex chaotic systems based on RBF neural network and sliding mode control. *Int. J. Mod. Phys. B* **2020**, *34*, 2050050. [CrossRef]
29. Fei-Fei, L.; Zhe-Zhao, Z. Synchronization of uncertain fractional-order chaotic systems with time delay based on adaptive neural network control. *Acta Phys. Sin.* **2017**, *66*, 090504. [CrossRef]
30. Luo, G.; Yang, Z.; Peng, K. Synchronizing chaotic systems with uncertain model and unknown interference using sliding mode control and wavelet neural networks. *Neural Process. Lett.* **2019**, *50*, 2547–2565. [CrossRef]
31. Wang, S. The synchronization of fractional chaotic systems with WRBF neural network. *Eur. Phys. J. Plus* **2022**, *137*, 945. [CrossRef]
32. Wang, S. A 3D autonomous chaotic system: Dynamics and synchronization. *Indian J. Phys.* **2024**, *98*, 4525–4533. [CrossRef]

Disclaimer/Publisher's Note: The statements, opinions and data contained in all publications are solely those of the individual author(s) and contributor(s) and not of MDPI and/or the editor(s). MDPI and/or the editor(s) disclaim responsibility for any injury to people or property resulting from any ideas, methods, instructions or products referred to in the content.